

[C II] EMISSION FROM NGC 4038/39 (THE “ANTENNAE”)

T. Nikola ^{1,2}, N. Geis ^{4,1}, R. Genzel ¹, F. Herrmann ¹, S.C. Madden ^{1,3}, A. Poglitsch ¹,
G.J. Stacey ⁵, C.H. Townes ⁴

¹ *Max-Planck-Institut für extraterrestrische Physik, Garching, Germany*

² *University of New South Wales, Sydney, Australia*

³ *CE-Saclay, Service d’Astrophysique, Gif-sur-Yvette, France*

⁴ *Department of Physics, University of California, Berkeley, USA*

⁵ *Department of Astronomy, Cornell University, Ithaca, USA*



Abstract

We present observations of NGC 4038/39 in the [C II] 158 μm fine structure line taken with the MPE/UCB Far-infrared Imaging Fabry-Perot Interferometer (FIFI) on the Kuiper Airborne Observatory (KAO). A fully sampled map of the galaxy pair (without the tidal tails) at 55'' resolution has been obtained. The [C II] emission line is detected from the entire galaxy pair and peaks at the interaction zone. The main part of the [C II] emission probably arises from photodissociation regions (PDRs). For standard conditions only a small part of the observed [C II] emission may come from the cold neutral medium (CNM). However, on the assumption of high temperature and high density in the CNM up to about one third of the observed [C II] emission may originate from the CNM. A comparison with single dish CO observations of the Antennae shows a [C II] to CO intensity ratio at the interaction zone a factor of 3 lower than usually observed in starburst galaxies, but still a factor of about 1.3 to 1.4 higher than at the nuclei of NGC 4038/39. Therefore, no global starburst is taking place in the Antennae. [C II] emission arising partly from confined starburst regions and partly from surrounding quiescent clouds could explain the observed [C II] radiation at the interaction zone, whereas toward the nuclei the star formation activity is generally low.

1 Introduction

The galaxy pair NGC 4038/39 (Arp 244) is an interacting system in an early stage of merging at a distance of about 21 Mpc from our own galaxy.

For the Antennae system as a whole only a relatively low star forming efficiency (only 3 times higher than in the Milky Way) has been found [20].

However, measurements in the radio continuum at 1.5 GHz and 4.9 GHz [6] and interferometric observations in the CO (1 → 0) Line [14] show clear evidence for strong ongoing star formation activity.

Recent observations of NGC 4038/39 with ISO [17, 7] also revealed strong star formation activity at the interaction zone.

An excellent tracer of star formation activity in galaxies is the strong [C II] 158 μm $^2\text{P}_{3/2} \rightarrow ^2\text{P}_{1/2}$ fine structure line which arises mainly from photodissociation regions (PDRs) created by far-ultraviolet photons from hot young stars impinging on nearby dense interstellar clouds [3, 12]. In combination with CO and farinfrared continuum (FIR) observations, the [C II] emission can be used with PDR models [16, 18, 19] to derive densities and far-UV (FUV) intensities and estimates of the star formation activity.

2 Observations

The observations of the Antennae in the [C II] $^2\text{P}_{3/2} \rightarrow ^2\text{P}_{1/2}$ fine structure line at 157.7409 μm have been carried out with the Kuiper Airborne Observatory (KAO) using the MPE/UCB Far-infrared Imaging Fabry-Perot Interferometer (FIFI; [11, 13]). We mapped an area of $300'' \times 300''$ including both galaxies and the interaction zone. At 158 μm the FWHM of the beam is about $55''$. We chose a spectral resolution of 144 km s^{-1} (FWHM) and a scan width of 380 km s^{-1} with the scan center at 1600 km s^{-1} . The wavelength calibration was implemented by means of the H₂S absorption line at 157.7726 μm . Flat fielding of the array was carried out with two internal black bodies. The secondary mirror of the telescope was chopped approximately $4'$ in roughly the east-west direction, and the telescope was nodded to compensate for the beam offset. For absolute intensity calibration we observed Jupiter at 158 μm and assumed a temperature of 128 K at this wavelength [5], an equatorial diameter of $43.22''$, and a pole diameter of $40.42''$ [2] for Jupiter. The accuracy of the intensity calibration is estimated to be about 30 % and the absolute pointing positions are uncertain by about $15''$.

3 Results

3.1 Spatial Distribution of the [C II] Emission

We superimposed the map of the [C II] 158 μm line emission on a short-exposed optical image of the Antennae [8] (Fig. 3.1). The contour levels are in steps of 1σ , $8.4 \times 10^{-6} \text{ erg s}^{-1} \text{ cm}^{-2} \text{ sr}^{-1}$, starting at the 1σ level. [C II] emission is seen over the full extent of the merging system and peaks at the interaction zone.

Taking the beam size into account, the [C II] emission agrees very well with the overall form of the galaxy pair as seen in the short-exposed optical image. The emission is elongated along the bridge between the two galaxies, including the interaction zone, NGC 4039, and extends even further south. It is also extended in the north-west showing the western loop of H II regions around NGC 4038.

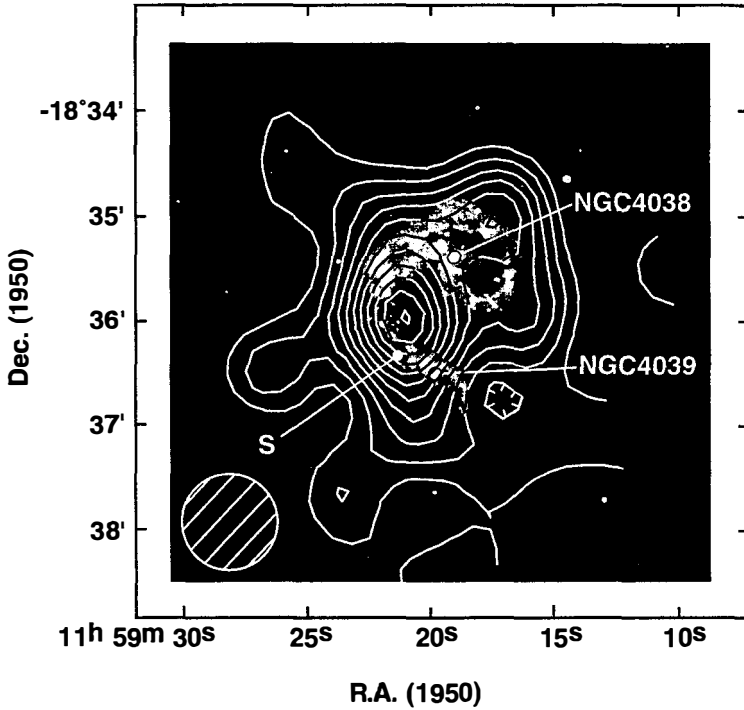


Figure 1: Integrated [C II] $158 \mu\text{m}$ intensity map of NGC 4038/39 superimposed on an optical image [8]. The contour levels are in steps of 1σ ($8.4 \times 10^{-6} \text{ erg s}^{-1} \text{ cm}^{-2} \text{ sr}^{-1}$) starting at the 1σ level. The symbol “S” indicates the southern clump of the CO emission at the interaction zone [14]. The hatched circle indicates the beam (FWHM of $55''$).

3.2 The [C II] Emitting Region

The results of the measurement of the [C II] $158 \mu\text{m}$ emission are given in Table 1. The total [C II] luminosity from the region enclosed by the first contour line in Fig. 3.1 is $L_{[\text{CII}]} = 2.9 \times 10^8 L_{\odot}$.

Assuming high temperature ($T \gg 91 \text{ K}$), high density ($n \gg n_{\text{crit}} = 3.5 \times 10^3 \text{ cm}^{-3}$), optically thin [C II] emission, and a beam filling factor of unity we can estimate a lower limit of the C^+ column density and hydrogen mass [3]. Using a solar fractional carbon abundance of $[\text{C}]/[\text{H}] \sim 3 \times 10^{-4}$ and assuming that all the carbon is in the form of C^+ we derive a lower limit of the hydrogen column density. The result of this estimate is given in Table 1.

For the whole Antennae system we estimated the FIR continuum from the IRAS flux densities at $60 \mu\text{m}$ and $100 \mu\text{m}$ [15] using the method given in [9]. We obtained a FIR luminosity for the whole system of $L_{\text{FIR}} = 3.6 \times 10^{10} L_{\odot}$. Consequently the total [C II] luminosity is about 0.8 % of the FIR luminosity. No FIR continuum map with a resolution comparable to the [C II]

Table 1: Results of the [C II] observation

Source	$I_{[\text{CII}]}$ ^a	$M_{\text{min}}(\text{H})$ $10^7 M_{\odot}$	$N_{\text{min}}(\text{H})$ 10^{20}cm^2	$L_{[\text{CII}]}$ $10^8 L_{\odot}$	L_{FIR} $10^{10} L_{\odot}$
[C II]-peak (interaction zone)	9.2	5.4	1.8		2.0
NGC 4038	4.4	2.7	0.88		1.4
NGC 4039	5.0	2.9	1.0		0.8
total galaxy pair		14.8	5.3 (average)	2.9	3.6

^a) Integrated [C II]-intensity in units of $10^{-5} \text{ erg s}^{-1} \text{ cm}^{-2} \text{ sr}^{-1}$.

data exists for the Antennae. Since the FIR continuum and the 20 cm radio continuum [6] of the whole Antennae system obey the FIR/radio correlation and with the assumption that the FIR/radio correlation is also valid at the scale of our beam size, we estimated the FIR continuum at the interaction zone and the nuclei by distributing the FIR continuum of the whole Antennae system the same way as the low spatial resolution 20 cm radio continuum [6]. For that we convolved the 20 cm map to a spatial resolution of $55''$ and scaled it such that the total flux in the map matches the IRAS observation. The obtained FIR luminosity of the interaction zone and of the nuclei NGC 4038/39 is given in Table 1.

4 Origin of the [C II] Radiation

The [C II] $158 \mu\text{m}$ fine structure line may arise from at least three components of the interstellar medium: photodissociation regions (PDRs), atomic gas clouds, and ionized medium. In starburst galaxies and star forming regions the contribution of the [C II] fine structure line from PDRs is much stronger than from the other components of the interstellar medium which can therefore be neglected. The possible contribution of [C II] emission from warm neutral medium (WNM) and from ionized medium (from H II regions and from extended low density warm ionized medium: ELDWIM) to the observed [C II] emission of the Antennae is negligibly small [10]. Under normal conditions of the CNM ($T = 70 \text{ K}$, $n_{\text{H}} = 100 \text{ cm}^{-3}$) the contribution of the [C II] emission to the observed integrated [C II] intensity is also small. However, for high temperature ($T = 100 \text{ K}$) and high density ($n_{\text{H}} = 200 \text{ cm}^{-3}$) the [C II] emission from CNM may rise to 1/3 of the observed integrated [C II] intensity [10].

4.1 [C II] Emission From PDRs

PDRs are the interfaces between H II regions and molecular clouds where photons with energies less than 13.6 eV escape from the H II regions, dissociate molecules and ionize elements with dissociation or ionization energies lower than the Lyman limit (13.6 eV). Carbon is the most abundant element with an ionization energy (11.3 eV) less than 13.6 eV. Ionized carbon is then excited by collisions with electrons and/or atomic and molecular hydrogen. The gas in the PDR is heated mainly by photoelectric emission from grains illuminated by FUV radiation. However, most of the FUV flux which is absorbed by grains is converted into FIR radiation.

To derive the density and the intensity of the FUV field in PDRs we used the model described in [12]. From the comparison of the [C II] integrated intensity with the derived FIR continuum and the intensity of the CO ($1 \rightarrow 0$) line [1] we obtain two possible solutions for the density

Table 2: Results of the PDR-model

Source	PDR-solution ^a	n_{H} [cm^{-3}]	$\chi_{\text{FUV}}^{\text{b}}$	$\Phi_{\text{b}}^{\text{c}}$
interaction zone ([CII]-Peak)	l	2.2×10^2	140	0.65
	h	1.5×10^5	480	0.19
NGC 4038	l	1.0×10^2	120	0.50
	h	3.2×10^5	500	0.12
NGC 4039	l	2.0×10^2	80	0.47
	h	1.3×10^5	250	0.14

a) l: low density solution for the PDRs

h: high density solution for the PDR

b) intensity of the FUV field in units of the interstellar radiation field: $\chi_{\text{o}} = 2 \times 10^{-4} \text{ erg s}^{-1} \text{ cm}^{-2} \text{ sr}^{-1}$ [4]

c) beamfilling factor: $\Phi_{\text{b}} = \frac{\chi_{\text{FIR}}}{\chi_{\text{UV}}}$

and the intensity of the FUV field χ_{FUV} for the PDR (Table 2). The CO data [1] support the high density solution for the interaction zone. For the nuclei of NGC 4038/39 none of the PDR solutions can be rejected. From the PDR model we also estimated the beamfilling factor given by $\Phi_{\text{b}} = \frac{\chi_{\text{FIR}}}{\chi_{\text{UV}}}$ (Table 2).

For starburst galaxies a [C II]/CO(1 \rightarrow 0) ratio of 6000 has been found while the more quiescent regions show a ratio of ~ 2000 [12]. Using the CO data from [1] we find [C II]/CO ratios of ~ 1900 at the [C II] peak (overlap region) and 1300 to 1400 toward the nuclei, implying there is no starburst activity taking place, given the resolution of our data.

By comparing the interferometric and the single dish CO measurements we constructed a two-component model with a confined starburst region and a quiescent surrounding molecular cloud system. Applying this model to our [C II] data we find that at the interaction zone a confined starburst with a [C II]/CO ratio of 6000 and a quiescent underlying medium with a [C II]/CO ratio of 500 could also explain our data. For the nuclei we found a lower star formation activity ([C II]/CO ratios of 3300 and 4700 for NGC 4038 and NGC4039, respectively) for a possible confined star forming region.

5 Conclusion

We present a map of NGC 4038/39 in the [C II] 158 μm fine structure line. [C II] emission is detected over the optical extent of the system of galaxies and peaks at the interaction zone. We derived minimum hydrogen masses and minimum column densities for the [C II] emitting regions. With the assumption that the FIR/radio correlation is valid at the scale of our beam size we estimated the FIR continuum at the interaction zone and the nuclei of NGC 4038/39 by distributing the FIR continuum of the whole Antennae system the same way as the 20 cm radio continuum. Using the FIR/radio correlation we estimated FIR luminosities for the interaction zone and the nuclei of the galaxies. The [C II] emission arises mainly from PDRs. Only at extreme conditions of the CNM a significant part (1/3) of the observed [C II] emission may originate in CNM. From the PDR model we obtained densities, intensities of the UV-field and beamfilling factors of the PDRs. We found that no global star formation is taking place in the

Antennae system. However, by constructing a two component model for the PDRs we showed that a confined strong starburst at the interaction zone and less strong star formation activity in the nuclei of NGC 4038/39 can explain our [C II] data.

Acknowledgements. We are grateful to the staff of the KAO for their competent support. This work was partially supported by the NASA grant NAG-2-208 to the University of California, Berkeley. N.G. was supported in part by a Feodor-Lynen-fellowship of the Alexander von Humboldt foundation.

References

- [1] Aalto, S., Booth, R.S., Black, J.H., & Johansson, L.E.B., 1995, *Astr. Astrophys.* **300**, 369
- [2] Astronomical Almanac 1992
- [3] Crawford, M.K., Genzel, R., Townes, C.H., & Watson, D.M., 1985, *Astrophys. J.* **291**, 755
- [4] Draine, B.T., 1978, *Astrophys. J. Suppl. Ser.* **36**, 595
- [5] Hildebrand, R.H., Loewenstein, R.F., Harper, D.A., Orton, G.S., Keene, J., & Whitcomb, S.E., 1985, *ICARUS* **64**, 64
- [6] Hummel, E., & van der Hulst, J.M., 1986, *Astr. Astrophys.* **155**, 151
- [7] Kunze, D. *et al.* 1996, *Astr. Astrophys.* **315**, L101
- [8] Laustsen, S., Madsen, C., & West, R.M., 1987 in: *Exploring The Southern Sky*, Springer-Verlag Berlin Heidelberg New York London Paris Tokyo
- [9] Lonsdale, C.J., Helou, G., Good, J.C., & Rice, W., 1985, *Cataloged Galaxies and Quasars Observed in the IRAS Survey*, (Pasadena: Jet Propulsion Laboratory)
- [10] Nikola, T., Geis, N., Genzel, R., Herrmann, F., Madden, S.C., Poglitsch, A., Stacey, G.J., Townes, C.H., submitted to *Astrophys. J.* ,
- [11] Poglitsch, A., Beeman, J.W., Geis, N., Genzel, R., Haggerty, M., Haller, E.E., Jackson, J., Rumitz, M., Stacey, G.J., & Townes, C.H., 1991, *Int. J. IR Millimeter Waves* **12**, 895
- [12] Stacey, G.J., Geis, N., Genzel, R., Lugten, J.B., Poglitsch, A., Sternberg, A., & Townes, C.H., 1991, *Astrophys. J.* **373**, 423
- [13] Stacey, G.J., Beeman, J.W., Haller, E.E., Geis, N., Poglitsch, A., & Rumitz, M., 1992, *Int. J. Millimeter Waves* **13**, 1689
- [14] Stanford, S.A., Sargent, A.I., Sanders, D.B., & Scoville, N.Z., 1990, *Astrophys. J.* **349**, 492
- [15] Surace, J.A., Mazzarella, J., Soifer, B.T., & Wehrle, A.E., 1993, *Astron. J.* **105**, 864
- [16] Tielens, A.G.G.M., & Hollenbach, D., 1985, *Astrophys. J.* **291**, 722
- [17] Vigroux, L. *et al.* 1996, *Astr. Astrophys.* **315**, L93
- [18] Wolfire, M.G., Hollenbach, D., & Tielens, A.G.G.M., 1989, *Astrophys. J.* **344**, 770
- [19] Wolfire, M.G., Tielens, A.G.G.M., & Hollenbach, D., 1990, *Astrophys. J.* **358**, 116
- [20] Young, J.S., Kenney, J.D., Tacconi, L., Claussen, M.J., Huang, Y.L., Tacconi-Garman, L., Xie, S., & Schloerb, F.P., 1986, *Astrophys. J.* **311**, L17